

Production and characterization of LaMnO₃ thin films prepared by Sol–Gel technique

M. Faruk Ebeođlugil[✉]

Dumlupınar University, Dept. of Material Science and Engineering, Kirazpınar Mahallesi,
Tavşanlı Yolu 10-km, 43000 Merkez, Kütahya, Turkey
[✉]Corresponding author: mfaruk.ebeođlugil@dpu.edu.tr

Submitted: 21 February 2016; Accepted: 27 February 2017; Available On-line: 4 April 2017

ABSTRACT: In this study, lanthanum manganite (LaMnO₃) thin films were prepared by sol-gel method for magnet technology. With this context, precursor solutions with low contact angles were synthesized from all nitrate salts of the respective cations (La, Mn), using ethanol as solvent and acetyl acetone as chelating agents. A dense amorphous film was deposited on silicon (Si) substrate. Crystallization of the films was carried out at temperatures between 850 and 1000 °C. The thermal, phase, elemental, microstructural and magnetic properties of the obtained samples were determined by TG/DTA, FTIR, XRD, XPS, SEM and VSM. The results show that sustained perovskite polycrystalline films were grown on the [100]-oriented Si substrates. In addition, the films show ferromagnetic behavior.

KEYWORDS: LaMnO₃; Magnet technology; Sol-gel

Citation/Citar como: Ebeođlugil, M.F. (2017) “Production and characterization of LaMnO₃ thin films prepared by Sol–Gel technique”. *Rev. Metal.* 53 (2): e091. <http://dx.doi.org/10.3989/revmetalm.091>

RESUMEN: *Producción y caracterización de láminas delgadas de LaMnO₃ preparadas por la técnica de Sol-Gel.* Se prepararon películas delgadas de manganita de lantano (LaMnO₃) mediante el método Sol-gel para la tecnología del imán. Se sintetizaron soluciones precursoras con bajos ángulos de contacto a partir de sales de nitrato de los respectivos cationes (La, Mn), utilizando etanol como disolvente y acetyl acetona como agente quelante. Se depositó una película amorfa y densa sobre sustrato de silicio (Si). La cristalización de las láminas se llevó a cabo a temperaturas entre 850 y 1000 °C. El comportamiento térmico, especies químicas, microestructura y propiedades magnéticas se determinaron mediante TG / DTA, FTIR, XRD, XPS, SEM y VSM respectivamente. Los resultados muestran que láminas policristalinas de perovskita crecieron sobre los sustratos de Si orientados en el plano [100]. Finalmente, las láminas muestran un comportamiento ferromagnético.

PALABRAS CLAVE: LaMnO₃; Sol-gel; Tecnología magnética

ORCID ID: M. Faruk Ebeođlugil (<http://orcid.org/0000-0003-4979-7017>)

Copyright: © 2017 CSIC. This is an open-access article distributed under the terms of the Creative Commons Attribution License (CC BY) Spain 3.0.

1. INTRODUCTION

Ferroelectric materials offer a wide range of useful properties. These include ferroelectric hysteresis (used in nonvolatile memories), high permittivity's (used in capacitors), high piezoelectric effects (used in sensors, actuators and resonant wave devices such as radio-frequency filters), high pyroelectric coefficients (used in infra-red detectors), strong electro-optic effects (used in optical switches) and anomalous temperature coefficients of resistivity (used in electric-motor overload protection circuits) (Setter *et al.*, 2006). In addition, ferroelectrics can be made in a wide variety of forms, including ceramics, single crystals, polymers and thin films increasing their exploitability (Yamamoto, 2000). Perovskite ferroelectric materials all have the general chemical formula ABO_3 , where A and B are cations. Typically the A cation will be around 1.2–1.6 Å in radius (similar to the oxygen ions) whilst the B cations perovskite-type oxides have attracted great interest in both applied and fundamental areas of solid-state chemistry, physics, advanced materials and catalysis (Monterrubio-Badillo *et al.*, 2006). In this paper, $LaMnO_3$ has been synthesized by the sol–gel method using ethanol as solvent and characterized for determined thermal, physical, mechanical, magnetic property and structural properties.

2. MATERIALS AND METHODS

$LaMnO_3$ was synthesized by sol–gel method. Before coating process, ultrasonically cleaned substrate is spin coated in sol-gel solution and taken immediately into vertical furnace which is preheated at 550 °C in air. After the substrate preparation, the powder of $La(NO_3)_3 \cdot 6H_2O$ (Biochem) and $Mn(NO_3)_3 \cdot 9H_2O$ (Biochem) were first dissolved in ethanol separately. Then 3 ml of acetic acid and 1 ml

of ethanol was added to the precursors under magnetic stirring. After having the red transparent solution, it was stirred at room temperature for 12 h in air prior to coating process. Before coating process, wettability properties of the solution were determined using contact angle measurement machine (Meter-CAM 100, KSV Instruments Ltd.). The solution was spinned onto Si wafers to be thin film. A dense amorphous film is coated on Si substrate. After spin coating process, the obtained gel coatings were dried at 300 °C for 10 min, heat treated at 500 °C for 5 min and subsequently annealed at 850 °C for 60 minutes and 1000 °C for 60 minutes with 5 °C/min heating regime in air to obtain the final thin films.

Thermal analyses of the La- and Mn-based xerogel dried at 150 °C for 30 min in air were carried out using a DTG-60H Model Differential Thermal Analysis/ Thermogravimetric (DTA/TG) machine. Fourier Transform Infrared (FTIR) spectra of the solutions, gel and film samples were recorded using Perkin Elmer FTIR spectrometer. X-ray diffraction (XRD) patterns of the thin films were performed by using a Thermo-Scientific, ARL-K α diffractometer with a $CuK\alpha$ irradiation (wavelength, $\lambda = 0.15418$ nm). The thin film morphologies of the samples were observed by a field emission scanning electron microscope (FESEM, FEI Novanosem 650). All measurements were performed at room temperature. X-ray Photoelectron Spectroscopy (XPS) characterization of the films was carried out with a Thermo Scientific K-Alpha Surface Analysis. Magnetic properties of the sample were determined using a Dexing Magnet - Vibrating Sample Magnetometer (VSM).

3. RESULTS AND DISCUSSION

Figure 1 shows wetting angle images of La- and Mn-based solutions added acetic acid and ethanol (21°) and added acetic acid (44°). The measurements

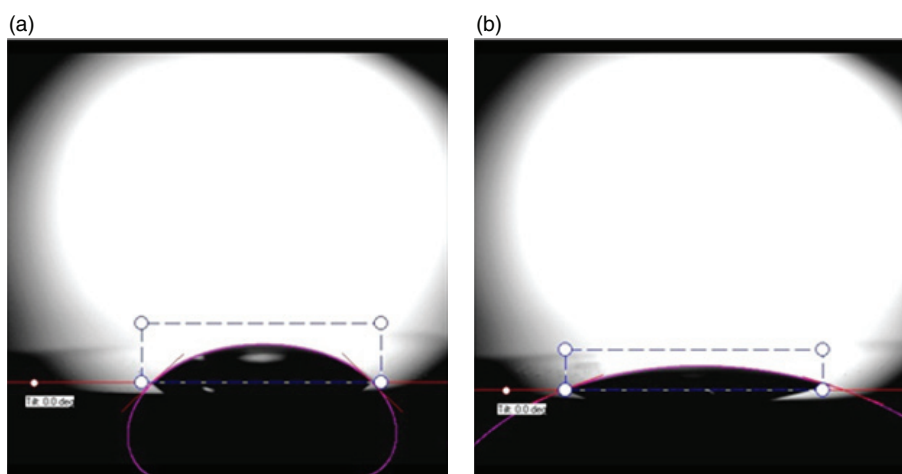


FIGURE 1. Wetting angle images of La- and Mn-based solutions: a) added acetic acid and ethanol (21°) and b) added acetic acid (44°).

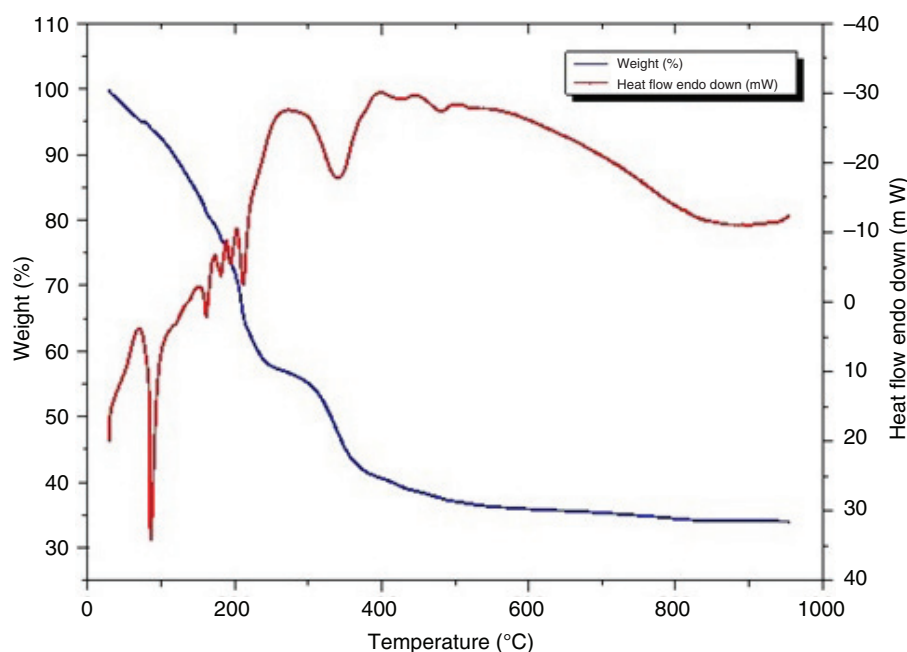


FIGURE 2. DTA and TGA curves of the sample obtained drying at 150 °C for 30 min in air from xerogel solution.

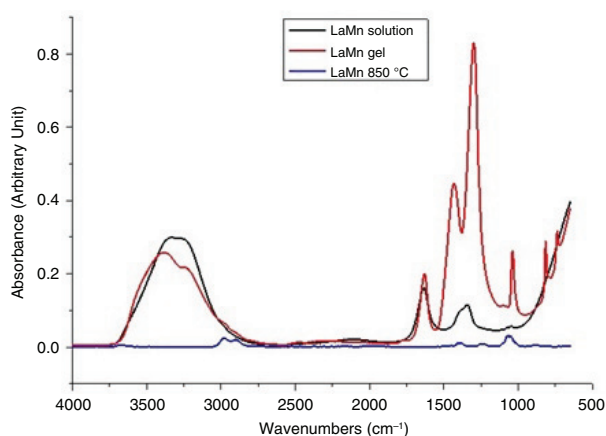


FIGURE 3. FTIR spectra of La- and Mn-based samples heat treated at 25 °C (as received from solution), 150 °C for 30 min (xerogel) and 850 °C.

showed that the contact angle values of La- and Mn- based solutions are in the range of 21° and 44°. Since the results are less than 90°, there is no inconsistency about wettability between substrates and solution.

DTA and TGA curves of the sample obtained drying at 150 °C for 30 min in air from xerogel solution is shown in Fig. 2. The sample was heated at regime of 5 °C min⁻¹ from 29 to 950 °C. The DTA curve exhibits one endothermic peak at 85 °C, two strong exothermic peaks at about 270, 390 °C and three weak exothermic peaks at about 180, 200 and 500 °C. The TG curve exhibits two major weight loss stages at the temperature ranges of 29–200 °C

and 200–450 °C. The first gradual weight loss step from 29 to 200 °C accompanying with a endothermic peak and a strong exothermic peak can be ascribed to the removal of the residual water and a partial decomposition of acetic acid and ethanol chain. The second weight loss stage at the temperature range of 200 and 450 °C accompanying with a weak exothermic peak corresponds to the decomposition of remaining organic matter and some of the nitrates. The remaining weight loss from 450 to 750 °C was accompanied with a small exothermic peak which can be attributed to the formation of the LaMnO₃ crystal. There is no weight loss above 850 °C. According to these, results, process temperatures such as combustion, oxidation and phase formation were chosen as 300 °C, 550 °C and 850–1000 °C, respectively (Gupta *et al.*, 1995).

The FTIR spectra of La- and Mn-based samples heat treated at 25 °C (as received from solution), 150 °C for 30 min (xerogel) and 850 °C which are recorded in the range 650–4000 cm⁻¹ are shown in Fig. 3. The broad absorption band at 3440 cm⁻¹ is associated with the O–H stretch of intermolecular hydrogen bonds or molecular water. The sharp absorption band at 1120 cm⁻¹ can be attributed to the vibrational mode of carbonates. The band at 855 cm⁻¹ corresponds to nitrate ions (Silva and Soares, 2009). The bands displacement is so light that it is only noticed when comparing spectra of calcined compounds at 400 and 850 °C. This may be due to the slight effect of temperature on the distribution of ions in the structure (Klvana *et al.*, 1997). The FTIR results supported to DTA-TG analysis.

Figure 4 presents XRD patterns of LaMnO_3 calcined at different temperatures characteristic peaks of the perovskite phase appear with low intensity, which signified the transformation of amorphous phase to the crystalline pure orthorhombic phase. XRD results reveal that the thicknesses of our as-deposited LaMnO_3 thin films 1000 (LM1000) and 850 (LM850) deposition cycles were respectively, with experimental errors around $\pm 5\%$. The thicknesses are correlated with the number of deposition cycles as expected, increasing with increasing number of deposition cycles such that growth per cycle could be calculated to be roughly 0.9 \AA/cycle . The small deviation from the perfectly linear dependence of the film thickness on the number of cycles is most probably due to minor changes in the reactor configuration. The dependence of crystal structure on the annealing temperature is illustrated in Fig. 4 where XRD patterns for variously annealed LM1000 thin films are shown. It can be seen that all these films exhibit a single-phase perovskite-type LaMnO_3 structure (Shimizu and Murata, 1997). The crystal structure is rhombohedral with space group R-3c. Even though determination of small variations in lattice parameters for thin-film samples is somewhat ambiguous we could see that the unit-cell volume for the LM1000 thin films increased (from 344.81 to 349.75 \AA^3) with annealing temperature increasing (Ni *et al.*, 2011). The films were fully crystallized after annealing at $1000 \text{ }^\circ\text{C}$. The XRD peaks of the annealed films

are given in Fig. 4 LaMnO_3 peaks appeared clearly after annealing at $1000 \text{ }^\circ\text{C}$ at two theta angles of 30 ; 32.8 ; 39.7 and 47.2 (Abrashev *et al.*, 1999).

The SEM technique was employed for finding morphology of LaMnO_3 as synthesized thin films heated at $850 \text{ }^\circ\text{C}$ and $1000 \text{ }^\circ\text{C}$. Figures 5 and 6 show SEM images of LaMnO_3 thin film heated at $850 \text{ }^\circ\text{C}$ and $1000 \text{ }^\circ\text{C}$ at different magnifications. One can notice the presence of macro-agglomerations of very fine particles on the surfaces having size less than $1 \mu\text{m}$. The particle shapes are not well defined. The coatings have micro cracks and pores. Many large and small pores are present in the whole material. We assume that the pores are mainly intergranular because intergranular pores can be seen on the SEM photographs. Coated film surfaces were also examined by means of SEM. The SEM examinations show that the film exhibits several microstructural defects and imperfections in a form of cracks and holes. The coating is homogeneous and the grains were distributed evenly (Silva and Soares, 2009).

Figure 7 shows XPS curve and results of LaMnO_3 heated at $850 \text{ }^\circ\text{C}$ respectively. In the LaMnO_3 the absence of peak in high energy value indicates the presence only of the lattice oxygen. Alterations in the crystalline structure and also in the electronic structure can be responsible for displacement of the peak in higher energy values. The Mn 2p spectra presents three signals which corresponds to Mn^{3+} (647.40 eV), Mn^{4+} (658.7 eV) and the presence of a peak, indicating the absence of Mn^{2+} . In LaMnO_3 film, the relation La/Mn is 0.79 , suggesting the

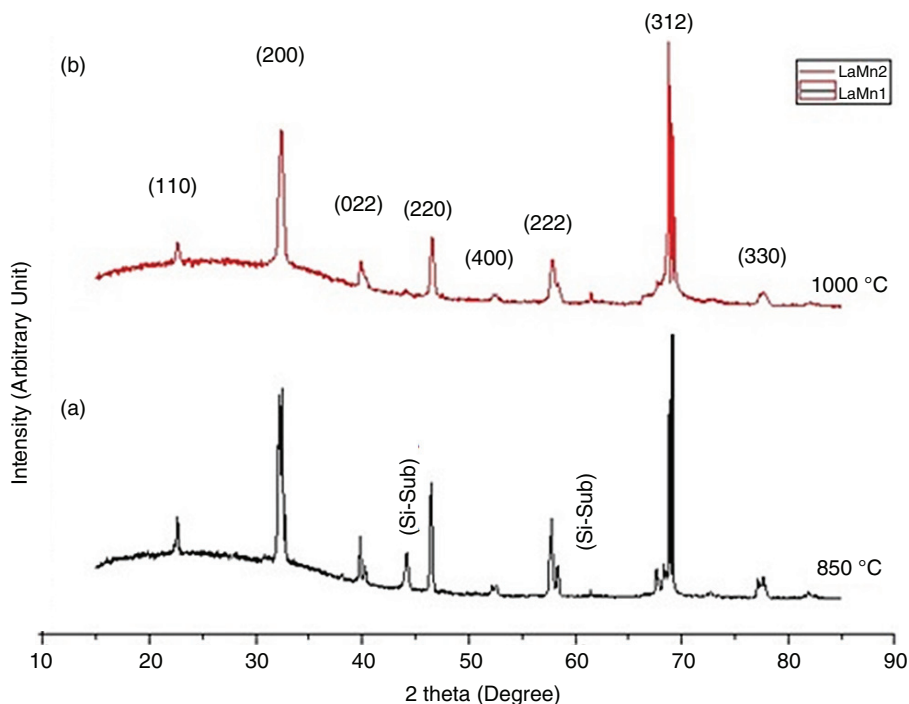


FIGURE 4. XRD patterns of the LaMnO_3 thin films annealed at: a) $850 \text{ }^\circ\text{C}$ and b) $1000 \text{ }^\circ\text{C}$ in air.

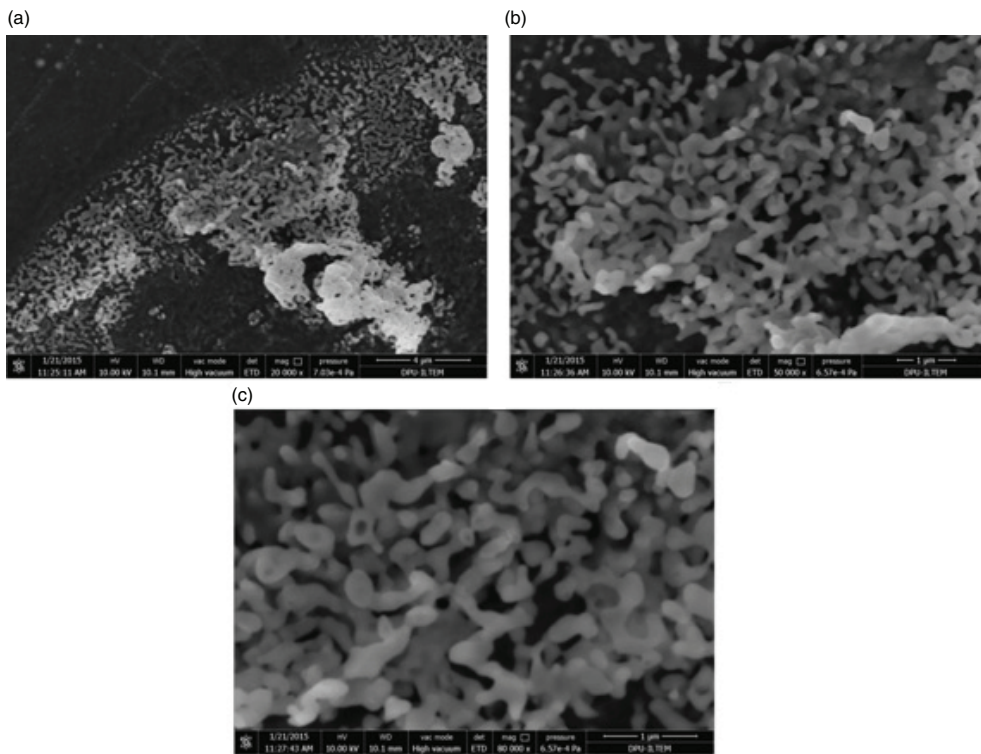


FIGURE 5. SEM images of LaMnO_3 thin film heated at $850\text{ }^\circ\text{C}$ at different magnifications such as: (a) 20000x, (b) 50000x and (c) 100000x.

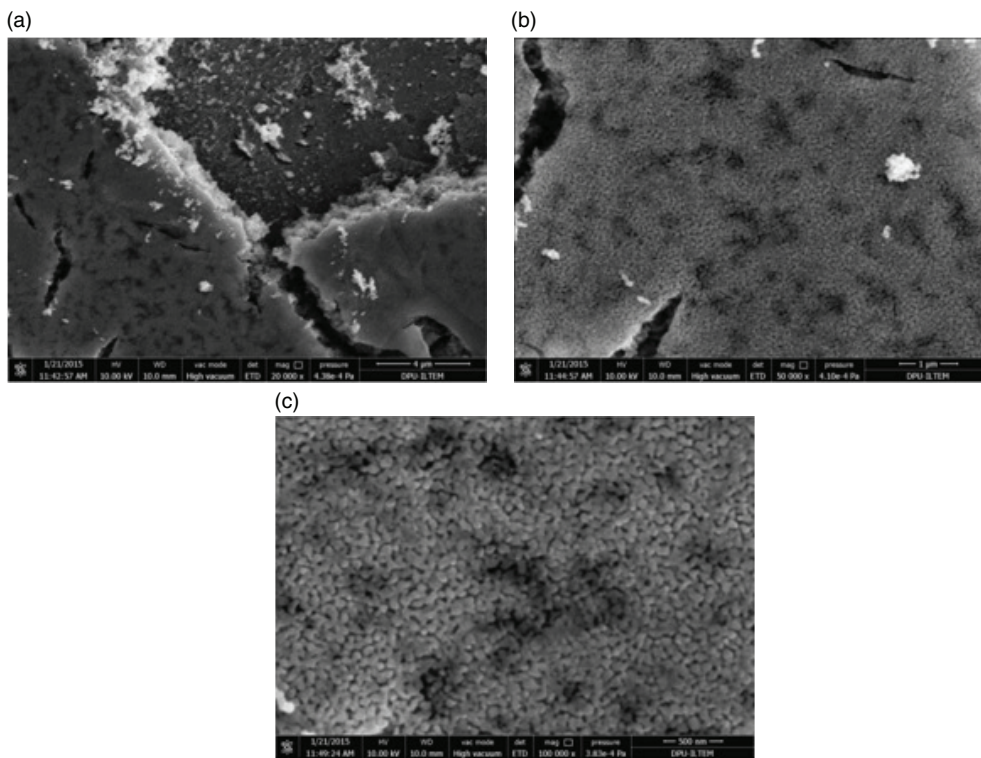
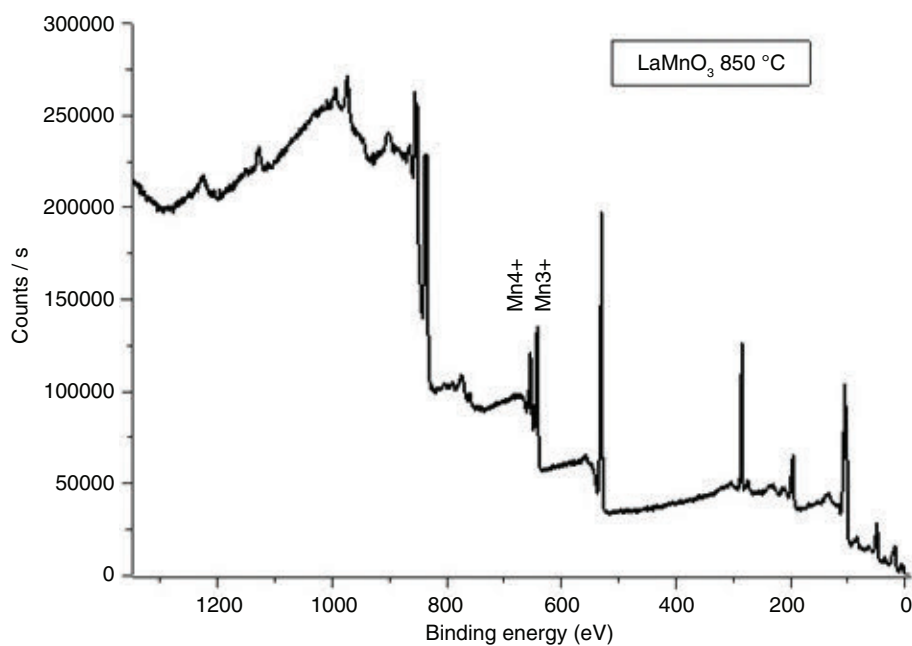
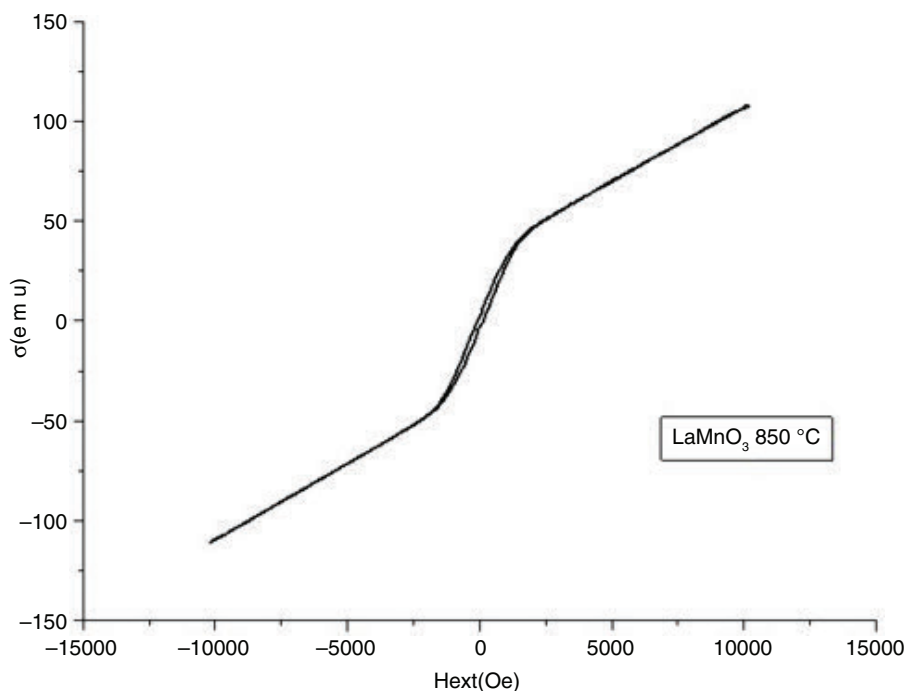


FIGURE 6. SEM images of LaMnO_3 thin film heated at $1000\text{ }^\circ\text{C}$ at different magnifications such as: (a) 20000x, (b) 50000x and (c) 80000x.

FIGURE 7. XPS curve of LaMnO₃ heated at 850 °C.FIGURE 8. VSM curve of LaMnO₃ sample heated at 850 °C.

non-stoichiometric LaMnO₃ phase with lanthanum deficiency (Raj Sankar and Joy, 2005). In order to keep the charge equilibrium, the conversion can be considered: Mn³⁺ to Mn⁴⁺. This transition comes with vacancies formation and presence of oxygen excess found the relation La/Mn changing from 1.5 to 2, depending on method used to obtain LaMnO₃. However, part of lanthanum isn't incorporated in

perovskite, but presented as oxide, and part of this oxide is carbonated (Zampieri *et al.*, 2002).

Hysteresis curve of magnetization were measured for the LaMnO₃ sample heated at 850 °C as shown in Fig. 8. The hysteresis loops at room temperature (300 K) were almost diamagnetic (Teraoka *et al.*, 2001; Brankovic *et al.*, 2010). However, below the transition temperature, the films show strong

ferromagnetic behavior, which is clear from Fig. 8. Annealing in O₂ atmosphere induces cation vacancies in LaMnO₃, which results in an up-shift of the magnetic transition temperatures and enhanced ferromagnetic character arising from the canting of the antiferromagnetic arrangement of spins (Gupta *et al.*, 1995; Ritter *et al.*, 1997; Nagai *et al.*, 2014; Yamaguchi *et al.*, 2016).

4. CONCLUSION

– Coating of ceramic films using sol-gel has promised in depositing dense and homogenous films for magnet technology. The deposited films cling to the substrate very well and the films exhibit several microstructural defects and imperfections in a form of cracks and holes. The coating is homogeneous and the grains were distributed evenly. Furthermore, the films show strong ferromagnetic behavior.

ACKNOWLEDGMENTS

This work was supported by Center for Fabrication and Applications of Electronic Materials (EMUM) and I specially thank to Prof. Dr. Erdal ÇELİK and Abdulvahid Çelebi for their help in this study.

REFERENCES

- Abrashev, M.V., Litvinchuk, A.P., Iliev, M.N., Meng, R.L., Popov, V.N., Ivanov, V.G., Chakalov R.A., Thomsen C. (1999). Comparative study of optical phonons in the rhombohedrally distorted perovskites LaAlO₃ and LaMnO₃. *Phys. Rev. B* 59 (6), 4146. <http://dx.doi.org/10.1103/PhysRevB.59.4146>.
- Brankovic, Z., Duris, K., Radojkovic, A., Bernik, S., Jaglicic, Z., Jagodic, M., Vojisavljevic, K., Brankovic, G. (2010). Magnetic properties of doped LaMnO₃ ceramics obtained by a polymerizable complex method. *J. Sol–Gel Sci. Technol.* 55 (3), 311–316. <http://dx.doi.org/10.1007/s10971-010-2251-4>.
- Gupta, A., McGuire, T.R., Duncombe, P.R., Rupp, M., Sun, J.Z., Gallagher, W., Xiao, G. (1995). Growth and giant magnetoresistance properties of La-deficient La_xMnO_{3–δ} (0.67 ≤ x ≤ 1) films. *Appl. Phys. Lett.* 67 (23), 3494–3496. <http://dx.doi.org/10.1063/1.115258>.
- Kivana, D., Delval, J., Kirchnerova, J., Chaouki, J. (1997). Deactivation of fiber-supported La_{0.65}Sr_{0.35}Ni_{0.29}Co_{0.69}Fe_{0.02}O₃ catalyst by mercaptan during combustion of methane or natural gas. *Appl. Catal. A Gen.* 165 (1–2), 171–182. [http://dx.doi.org/10.1016/S0926-860X\(97\)00199-3](http://dx.doi.org/10.1016/S0926-860X(97)00199-3).
- Monterrubio-Badillo, C., Ageorges, H., Chartier, T., Coudert, J.F., Fauchais, P. (2006). Preparation of LaMnO₃ perovskite thin films by suspension plasma spraying for SOFC cathodes. *Surf. Coat. Technol.* 200 (12–13), 3743–3756. <http://dx.doi.org/10.1016/j.surfcoat.2005.01.002>.
- Nagai, T., Fujiwara, N., Asahi, M., Yamazaki, S., Siroma, Z., Loroi, T. (2014). Synthesis of nano-sized perovskite-type oxide with the use of polyvinyl pyrrolidone. *J. Asian Ceram. Societies* 2 (4), 329–332. <http://dx.doi.org/10.1016/j.jascr.2014.08.004>.
- Ni, H., Yu, D., Zhao, K., Kong, Y.C., Wong, H.K., Zhao, S.Q., Zhang, W.S. (2011). Oxygen content dependence of the photovoltaic characteristic of miscut manganite thin films. *J. Appl. Phys.* 110 (3), 033112. <http://dx.doi.org/10.1063/1.3620984>.
- Raj Sankar, C., Joy, P.A. (2005). Magnetic properties of the self-doped lanthanum manganites La_{1–x}MnO₃. *Phys. Rev. B* 72, 024405. <http://dx.doi.org/10.1103/PhysRevB.72.024405>.
- Ritter, C., Ibarra, M.R., De Teresa, J.M., Algarabel, P.A., Marquina, C., Blasco, J., Garcia, J., Oseroff, S., Cheong, S.-W. (1997). Influence of oxygen content on the structural, magnetotransport, and magnetic properties of LaMnO_{3+δ}. *Phys. Rev. B: Condens. Matter.* 56 (14), 8902. <http://dx.doi.org/10.1103/PhysRevB.56.8902>.
- Setter, N., Damjanovic, D., Eng, L., Fox, G., Gevorgian, S., Hong, S., Kingon, A., Kohlstedt, H., Park, N.Y., Stephenson, G.B., Stolitchnov, I., Taganste, A.K., Taylor, D.V., Yamada, T., Streiffner, S. (2006). Ferroelectric thin films: Review of materials, properties, and applications. *J. Appl. Phys.* 100 (5), 051606. <http://dx.doi.org/10.1063/1.2336999>.
- Silva, P.R.N., Soares, A.B. (2009). Lanthanum based high surface area perovskite-type oxide and application in CO and propane combustion. *Ecl. Quím.* 34 (1), 31–38. <http://dx.doi.org/10.1590/S0100-46702009000100005>.
- Shimizu, Y., Murata, T. (1997). Sol–Gel Synthesis of Perovskite-Type Lanthanum Manganite Thin Films and Fine Powders Using Metal Acetylacetonate and Poly(vinyl alcohol). *J. Am. Ceram. Soc.* 80 (10), 2702–2704. <http://dx.doi.org/10.1111/j.1151-2916.1997.tb03178.x>.
- Teraoka, Y., Kanada, K., Kagawa, S. (2001). Synthesis of La K Mn O perovskite-type oxides and their catalytic property for simultaneous removal of NO_x and diesel soot particulates. *Appl. Catal. B-Environ.* 34 (1), 73–78. [http://dx.doi.org/10.1016/S0926-3373\(01\)00202-8](http://dx.doi.org/10.1016/S0926-3373(01)00202-8).
- Yamamoto, O. (2000). Solid oxide fuel cells: fundamental aspects and prospects. *Electrochim. Acta* 45 (15–16), 2423–2435. [http://dx.doi.org/10.1016/S0013-4686\(00\)00330-3](http://dx.doi.org/10.1016/S0013-4686(00)00330-3).
- Yamaguchi, S., Wada, H., Sánchez-Rodríguez, D., Farjas, J., Yahiro, H. (2016). Synthesis of perovskite-type oxide, LaFeO₃, from coordination polymer precursor, La[Fe(CN)₆]5H₂O. *J. Ceram. Soc. Jpn.* 124 (1), 7–12. <http://doi.org/10.2109/jcersj2.15198>.
- Zampieri, G., Abbate, M., Prado, F., Caneiro, A., Morikawa, E. (2002). XPS and XAS spectra of CaMnO₃ and LaMnO₃. *Physica B* 320 (1–4), 51–55. [http://dx.doi.org/10.1016/S0921-4526\(02\)00618-X](http://dx.doi.org/10.1016/S0921-4526(02)00618-X).